Photosynthetic Oxygen Evolution Is Not Reversed at High Oxygen Pressures: Mechanistic Consequences for the Water-Oxidizing Complex[†]

Derrick R. J. Kolling, Tyler S. Brown, Gennady Ananyev, and G. Charles Dismukes*

Department of Chemistry and Princeton Environmental Institute, Princeton University, Washington Road, Princeton, New Jersey 08544

Received September 17, 2008; Revised Manuscript Received December 2, 2008

ABSTRACT: We investigated the effects of elevated O_2 pressure on the production of O_2 by photosynthetic organisms in several species of plants, algae, and a cyanobacterium. Using a noninvasive fluorometry technique to monitor sequential turnover of the photosystem II (PSII) reaction center as a function of O_2 pressures, we showed that none of the reactions of water oxidation are affected by elevated O_2 pressures up to 50-fold greater than atmospheric conditions. Thus, the terminal step of O_2 release from the water oxidation complex ($S_4 \rightarrow S_0 + O_2 + nH^+$) is not reversible in whole cells, leaves, or isolated thylakoid membranes containing PSII, in contrast to reports using detergent-extracted PSII complexes. This implies that there is no thermodynamically accessible intermediate that can be populated by preventing or reversing the O_2 release step with O_2 at atmospheric pressure. To assess the sensitivity of PSII charge recombination to O_2 pressure, we quantitatively modeled the consequences of two putative perturbations to the catalytic cycle of water oxidation within the framework of the Kok model. On the basis of the breadth of oxygenic phototrophs examined in this study, we conclude that O_2 accumulation in cells or the atmosphere does not suppress photosynthetic productivity through the reversal of water oxidation in contemporary phototrophs and would have been unlikely to influence the evolution of oxygenic photosynthesis.

Oxygenic photosynthesis is the most successful form of biological energy metabolism on Earth today. In terms of biomass, it dominates our planet, being represented by all species of higher plants, algae, and cyanobacteria. Recent publications (*1*−*3*) and letters (*4*−*6*) have addressed a fundamental question of energy metabolism in these organisms: Is the production of O_2 by photosynthesis slowed or prevented at atmospheric pressures of O_2 that are or were formerly present on Earth? If the answer is yes, the consequences for the evolution of life on Earth are significant. Moreover, this question addresses the fundamental understanding of the chemistry of water oxidation by photosynthesis, which serves as a model for creating biomimetic catalysts for solar-to-chemical energy conversion.

Clausen et al. (*1, 2*) have given recent evidence that the last step in the four-step water oxidation reaction has an intrinsically low thermodynamic driving force (ΔG) and, thus, can be prevented by application of low O_2 pressure (50% suppression at 2.3 bar with an observable suppression beginning at atmospheric pressure). A consequence of their conclusion is that the rate of photosynthetic energy storage (proton-driven ATP production) would slow even at partial solar flux owing to charge recombination in O_2-blocked centers. This postulated loss of solar energy conversion efficiency could have slowed the evolution of oxygenic photosynthesis on early Earth (*7*). Other lines of historical evidence, which have been recently reviewed, have concluded that atmospheric O_2 has little if any effect on photosynthetic productivity under current atmospheric conditions (*3*). In contrast, inhibition of photosynthetic biomass accumulation due to illumination at elevated O_2 pressure does occur in photobioreactors (*8*), although the origin of this loss is believed to be dominated by O_2-sensitive photoinactivation rather than blocking of O_2 evolution (*9*).

To understand how O_2 pressure might possibly influence the chemistry of O_2 production, we must examine the catalytic site, the O_2-evolving complex (OEC),[1] located within a domain of the photosystem II (PSII) reaction center protein complex. In the overall reaction, four electrons and four protons are stripped from two water molecules to produce O_2. It has been known for 36 years that O_2 production requires a catalyst that accumulates four electron vacancies (oxidation equivalents or holes) formed upon four sequential light-driven charge separation reactions (*10, 11*). The yield of O_2 formed by the OEC upon exposure to individual short flashes is described by the standard Kok model. This model is a simple Markov chain that passes through five sequential oxidation states (S_0, S_1, S_2, S_3, S_4) that are populated by photon absorption. After S_4 forms, it spontaneously decays in the dark to form the initial state, S_0, by releasing O_2 (Figure 1A). The Kok model is shown in Figure 1A and includes two additional postulated inter-

[†] This work was supported by grants from the NIH (GM-39932) and NSF-IDBR (DBI-0138012). D.R.J.K. received support from the Camille and Henry Dreyfus Postdoctoral Fellowship in Environmental Chemistry and Donors of the American Chemical Society Petroleum Research Alternative Energy Fellowship.

* To whom correspondence should be addressed. E-mail: dismukes@princeton.edu. Phone: (609) 258-3949. Fax: (609) 258-1980.

[1] Abbreviations: PSII, photosystem II; OEC, O_2-evolving complex; FRRF, fast-repetition-rate fluorometry; XAS, X-ray absorption spectroscopy; DCMU, 3-(3,4-dichlorophenyl)-1,1-dimethylurea; *A. maxima*, *Arthrospira maxima*.

10.1021/bi801774f CCC: $40.75
Published on Web 01/23/2009

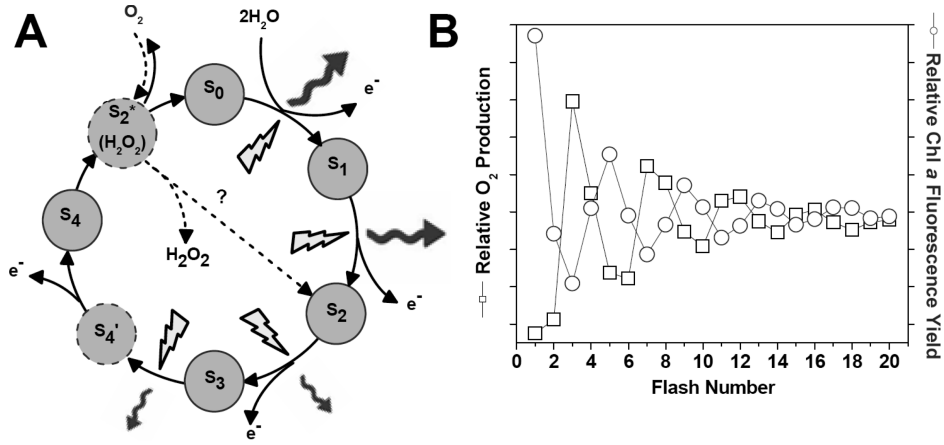

FIGURE 1: The S-state cycle and how to monitor it. (A) Scheme of intermediates (S-states) in the reaction cycle of photosynthetic water oxidation (i.e., the Kok model). Lightning bolts represent photon absorbance events (hits), and wavy arrows represent fluorescence emission (arrow size correlates with fluorescence quantum yield). Proton release events are omitted in this scheme. Recently proposed intermediates of the terminal reaction of the cycle are indicated with a dashed boundary (*5, 12*); also included is a hypothesized alternative pathway under elevated O_2 pressure (dashed arrows). (B) The PSII oxygen yield (○) and F_v/F_m (relative variable Chl-*a* fluorescence yield) (□) obtained from single-turnover flashes given to cells of *A. maxima*. Note that the two methods produce approximately "period four" oscillations, opposite in phase and with slightly different damping, reflecting S-state cycling.

mediates between S_3 and S_0 that have been proposed recently (see below).

Recent evidence suggests that the terminal step in O_2 evolution in which the O−O bond forms, $S_4 \rightarrow S_0 + nH^+ + O_2$, may proceed through an intermediate (*5, 12*). Time-resolved "pump-probe" X-ray absorption spectroscopy (XAS) capable of tracking Mn X-ray fluorescence changes with a time resolution of 10 μs has detected a transient intermediate that forms after photoexcitation of S_3 and before O−O bond formation (*12*). This intermediate was proposed to be a deprotonated S_3-state (denoted S_4'). It is important to note that the XAS data that support the existence of this intermediate at ambient pressure do not show evidence for or against a second intermediate (*12*), which was recently a point of contention (*4*−*6*).

Clausen and Junge proposed the formation of a different intermediate during $S_4 \rightarrow S_0$, an S_2-peroxo intermediate denoted $S_2^*(H_2O_2)$, in which the substrate water has been partially oxidized by two electrons (*1, 2*). This was postulated to form at elevated O_2 pressure and, unlike native S_4, was speculated to decay to the native S_2-state with release of H_2O_2, e.g., $S_4 \rightarrow S_2^*(H_2O_2) \rightarrow S_2 + H_2O_2$. This hypothesis was based on a decrease in the manganese UV absorbance change following photogeneration of S_4 under elevated O_2 pressures. To explain this result, it was proposed that an $S_2^*(H_2O_2)$ intermediate builds up at elevated O_2 pressure as a result of a shift in the equilibrium of the terminal reaction. It was also speculated that the $S_2^*(H_2O_2)$ intermediate could decay to S_2 upon liberation of H_2O_2 (*1*). Formation and decay of an intermediate were later supported by delayed fluorescence work done by Clausen et al. (*2*), although H_2O_2 was not detected as a product. Both of these possibilities have been included in the modified S-state cycle model represented in Figure 1A. The observed effect reached 50% of maximum at 2.3 bar and saturated between 14 and 30 bar. Their study was performed with detergent-extracted PSII core complexes from the cyanobacterium *Synechocystis* sp. PCC6803 and was supported by independent measurements of delayed chlorophyll *a* fluorescence using detergent-extracted PSII-enriched thylakoid membranes isolated from spinach (*2*). The formation of a native peroxide-like intermediate at S_2 has been postulated before (*13*−*16*), and H_2O_2 production has been observed from blocked PSII centers incapable of O_2 production or normal S-state turnover (*17, 18*). However, there has been no direct experimental support for a peroxo intermediate or O_2-bound product following S_4 in any PSII complex until the reports by Clausen et al.

In the present study, we have investigated O_2 production in all three major branches of oxygen-producing phototrophs at elevated O_2 pressures up to 10.3 bar (and up to 43 bar in *Arthrospira maxima*) using a noninvasive method that monitors chlorophyll fluorescence from intact cells (microalgae and cyanobacteria), plant leaves, and isolated thylakoid membranes. Our results show that none of the reactions of water oxidation, especially the terminal step ($S_4 \rightarrow S_0 + O_2 + nH^+$), are mechanistically affected by elevated O_2 pressures up to 50-fold greater than atmospheric conditions. Thus, the terminal reaction has no thermodynamically accessible peroxo or O_2-bound intermediate that can be populated by reversing the O_2 release step using elevated levels of O_2. The consequences for the mechanism of water oxidation are examined.

EXPERIMENTAL PROCEDURES

Sample Preparation. Subchloroplast membrane fragments (thylakoids) were isolated from market spinach following the method of Berthold et al. (*19*) with minor modifications as follows: a commercial juicing machine was employed for initial mechanical homogenization of the sample; material isolated after the second centrifugation step was used in the experiments. *A. maxima* cells were grown at 30 °C in complete Zarrouk medium at initial pH 9.0 and light intensity 40 μE m^{-2} s^{-1} and harvested just after the logarithmic phase of growth (6−8 days, pH 9.5). CO_2 bubbling was provided to replace inorganic carbon depleted from the growth medium through carbon fixation. Samples were suspended at 50 μg of Chl/mL and placed in shallow sample cuvette (~1.0 mm deep, 40 μL total volume). A "moat" surrounding the sample cuvette was filled with water to prevent sample dehydration during long measurement periods. For simultaneous O_2

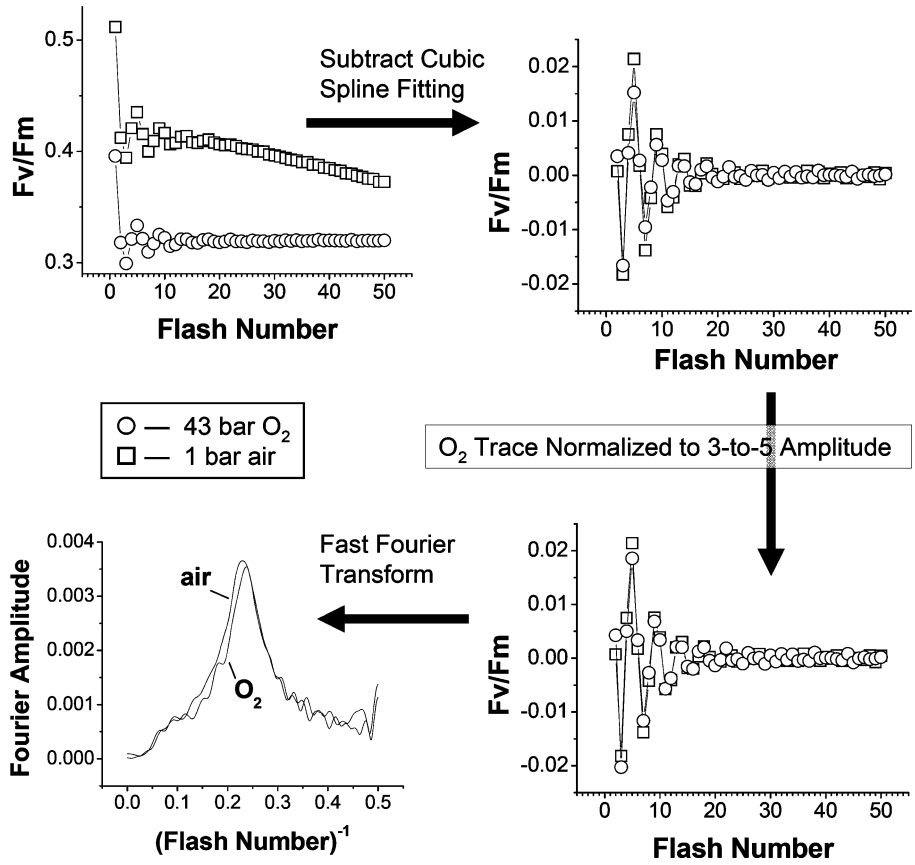

FIGURE 2: Data analysis of *A. maxima* F_v/F_m traces under 1 bar of air and 43 bar of O_2. The upper left panel of the figure shows F_v/F_m traces for *A. maxima* under atmospheric (□) and elevated O_2 conditions (○). The first point is removed from the trace, and it is then subtracted by a cubic spline fitting to result in the traces in the upper right panel. For comparison of the oscillations, the O_2 trace is then normalized to the air trace at the three-to-five flash amplitude. Finally, the fast Fourier transformation of both traces over the 50 flash interval is taken and shown in the lower left panel. Comparison of these results shows that there is little change in the Fourier amplitude and the period of the cycle upon exposure to 43 bar of O_2.

concentration and fluorescence yield experiments, whole cells of *A. maxima* were layered on a membrane-covered Clark-type Pt electrode at a thickness 0.3 mm and dark adapted for 5 min before flash illumination (*20*). *Dunaliella* sp. CCMP 1320 was grown at 25 °C in f/2 medium that was not supplemented with silica (http://www-cyanosite.bio.purdue.edu/media/table/f2.html).

Fluorescence Measurements. A stainless steel measurement cell, capable of holding pressures up to 40 bar for 24−48 h, was built to adapt the existing FRR fluorometer (*21*) for high-pressure measurements. The home-built FRR fluorometer is an accurate, versatile instrument that enables a wide range of chlorophyll fluorescence measurements. A laser diode excitation source ($\lambda_{max} = 655$ nm) provides sharp, stable pulses at a maximum light intensity of 32000 μE m^{-2} s^{-1}. In typical single-turnover excitation experiments, a train of 25 identical pulses, each 1 μs in duration followed by a 1 μs dark interval, induces chlorophyll *a* fluorescence at 680−690 nm to rise from its initial level after dark adaption (F_0) to a saturated state (F_m); the flash train thus constitutes a single-turnover flash in which 100% of the primary acceptor Q_A is reduced to Q_A^-. Repeating single-turnover flashes at 10−100 Hz produces transient period four oscillations in the yield of variable fluorescence (F_v/F_m), indicating modulation from the donor side S-state cycle.

Analysis of F_v/F_m Data. Signal averaging of flash sequences was performed to improve S/N ratio. Dark adaptation between signal coadditions was chosen to ensure recovery of the initial S-state populations characteristic of the dark stable populations. Averaging was done over 24 h for atmospheric conditions, while 2 h was the upper limit used for elevated O_2 conditions. We compared the rate of damping of F_v/F_m oscillations that were produced by 50 saturating flashes starting with dark-adapted samples by using the following analysis (the procedure is demonstrated in Figure 2): For the purpose of analyzing the oscillations, it is standard practice to remove the first flash response from all samples as this includes noncycling PSII centers (*21*). Then, the nonoscillating baseline was subtracted from all traces using a cubic spline fit. To compare the effect of elevated O_2 on the rate of damping of the F_v/F_m oscillations between samples, it was essential to compensate for the signal loss arising from inactivation of centers caused by superoxide in the samples that builds up upon exposure to elevated O_2 and light (this slow cumulative effect is included due to the 2 h window used for averaging). This was accomplished by normalizing the trace from the oxygen-treated sample to the atmospheric pressure sample by using the three-to-five flash amplitude. Finally, the fast Fourier transformation algorithm was then performed to obtain the frequency components responsible for the decay in amplitude from dephasing of S-states. The lowest frequency attainable by our analysis is 0.5 flash number^{-1}, which corresponds to a period of two flashes. This is a mathematical limitation and is due to the fact that it is impossible to use a flash number below 2 in the experiment. Regardless, if a component of period two

were present in our data, it would be observable as a shoulder at period two. Data were plotted in Origin 7.0, and Fourier transformations were performed in software written by Andrei Astashkin (University of Arizona, Tucson, AZ). Kok model fittings were performed in Origin 7.0 using an algorithm reported by Shinkarev (*22*).

Traditionally, S-state cycling data are analyzed using the Kok model (*11, 22, 23*). However, deviations from progressing through four sequential S-states (e.g., skipping S_1 with an $S_2^*(H_2O_2) \rightarrow S_2$ shunt, Figure 1A) would cause the symmetry in the model to be broken and require additional parameters in an already underdetermined model (*22*−*24*). To bypass these difficulties, FRRF data were analyzed by fast Fourier transform to characterize the frequency spectrum of the variable fluorescence yield (F_v/F_m) upon S-state cycling. This model-independent approach eliminates the assumptions implicit in the Kok model, as it simply relies on measuring the different intensities of the oscillating components of F_v/F_m produced during S-state cycling.

Simulation of F_v/F_m Data. A simple Markov model was implemented in MatLab 7.4.0 to generate the simulation. For the Kok model, the following equation was used:

$$\begin{bmatrix} S_1 \\ S_2 \\ S_3 \\ S_0 \end{bmatrix} = \begin{bmatrix} S_0 & S_3 & S_1 \\ S_1 & S_0 & S_2 \\ S_2 & S_1 & S_3 \\ S_3 & S_2 & S_0 \end{bmatrix} \begin{bmatrix} 1-\alpha-\beta \\ \beta \\ \alpha \end{bmatrix} - \begin{bmatrix} 0 \\ 0 \\ 0 \\ 0 \end{bmatrix}$$

where α and β represent misses and double hits, respectively.

For the shunt model, the following equations were used:

$$\begin{bmatrix} S_1 \\ S_2 \\ S_3 \\ S_0 \end{bmatrix} = \begin{bmatrix} S_0 & S_3 & S_1 \\ S_1 & S_0 & S_2 \\ S_2 & S_1 & S_3 \\ S_3 & S_2 & S_0 \end{bmatrix} \begin{bmatrix} 1-\alpha-\beta \\ \beta \\ \alpha \end{bmatrix} - \begin{bmatrix} 0 \\ -S_3(1-\alpha-\beta)\delta - S_2\beta\delta \\ 0 \\ S_3(1-\alpha-\beta)\delta + S_2\beta\delta \end{bmatrix}$$

where α and β represent misses and double hits, respectively, and δ represents the percentage of centers undergoing the $S_3 \rightarrow S_2$ shunt.

For the inactivation model, the following equations were used:

$$\begin{bmatrix} S_1 \\ S_2 \\ S_3 \\ S_0 \end{bmatrix} = \begin{bmatrix} S_0 & S_3 & S_1 \\ S_1 & S_0 & S_2 \\ S_2 & S_1 & S_3 \\ S_3 & S_2 & S_0 \end{bmatrix} \begin{bmatrix} 1-\alpha-\beta \\ \beta \\ \alpha \end{bmatrix} - \begin{bmatrix} 0 \\ 0 \\ 0 \\ S_3(1-\alpha-\beta)\gamma + S_2\beta\gamma \end{bmatrix}$$

where α and β represent misses and double hits, respectively, and γ represents the percentage of centers that during the $S_3 \rightarrow S_0$ step, undergo an inactivation.

The sum of the S_1 and S_0 populations was then determined per theoretical flash. These populations were subjected to an iterative process where results from one theoretical flash were used to generate results for the next theoretical flash.

RESULTS

The light intensity-dependent chlorophyll *a* fluorescence yield, called variable fluorescence (F_v), is sensitive to both the redox state of the Mn_4Ca cluster (i.e., the S-state) and the redox state of the primary quinone acceptor (Q_A) (*25*−*27*). This sensitivity has been widely used to monitor the yield and kinetics of turnover of PSII (*28, 29*). Using laser-based fast-repetition-rate fluorometry (FRRF) (*21*), we monitored the yield of prompt chlorophyll *a* fluorescence arising from photon emission using short (single-turnover) flashes that saturate the yield of charge separation. Starting with dark-adapted samples, the fluorescence yield on each flash rises from a low level observed in samples with open PSII centers (F_o) to a maximum level in closed centers (F_m). The ratio of the variable to maximum fluorescence yields, $(F_m - F_o)/F_m$, denoted by F_v/F_m, is proportional to the PSII charge-separation quantum efficiency (*21, 29*). A representative example is shown in Figure 2A. It is useful to note that F_v/F_m is an intensive variable and, thus, is independent of sample size.

The accuracy with which FRRF can monitor the S-state cycle is illustrated in Figure 1B, which shows that when a series of flashes is given to a dark-adapted sample, F_v/F_m oscillates 180° out of phase with the O_2 yield (measured electrochemically via a fast Clark electrode) (*21*). The approximately period four oscillation arises because the resulting fluorescence from the reaction center depends upon the S-state of the OEC (*26*). Laser-based FRRF thus provides an alternative method to monitor S-state cycling that works well at very high flash repetition rates and with intact phototrophs, unlike oximetry which relies on O_2 diffusion to an external electrode and thus is limited to about 5 Hz flashing rates and protein or cellular suspensions. O_2 detection using a bare Pt electrode and thin film samples also has fast resolution but requires electrochemical biasing of the sample at a reducing potential (Joliot-type electrode). This biasing produces H_2O_2 which alters the S-state distribution and eventually inactivates the sample (*30*). Another benefit of FRRF, and essential to the basis of this paper, is that high levels of O_2 do not directly interfere with the detection of chlorophyll *a* fluorescence as opposed to electrochemical detection of O_2. Oxygen electrodes are quickly saturated at the O_2 pressures used within this study.

High-Pressure O_2 Data. To record the intrinsic effect that O_2 pressure has on water oxidation chemistry *in vivo*, we examined living cells and leaves under otherwise physiologically relevant conditions following dark adaptation to achieve a population of the dark stable S-states. Samples consisted of a cyanobacterium, *A. maxima* CS328, a marine alga, *Dunaliella* sp. CCMP 1320, a freshwater alga *Chlamydomnas reinhardtii*, and several higher plant species: spinach, white clover, ginkgo, *Euonimus* sp., and sugar maple (Figures 2 and 3 and Table 1). We also obtained data from a subcellular sample of native spinach thylakoid membranes which were isolated without using detergents (Figure 3 and Table 1). We were unable to obtain high-quality F_v/F_m data on detergent-extracted PSII protein and detergent-fractionated PSII-enriched thylakoid membranes (like those used in refs *1* and *2*, respectively) due to higher background chlorophyll *a* fluorescence from free or uncoupled chlorophyll.

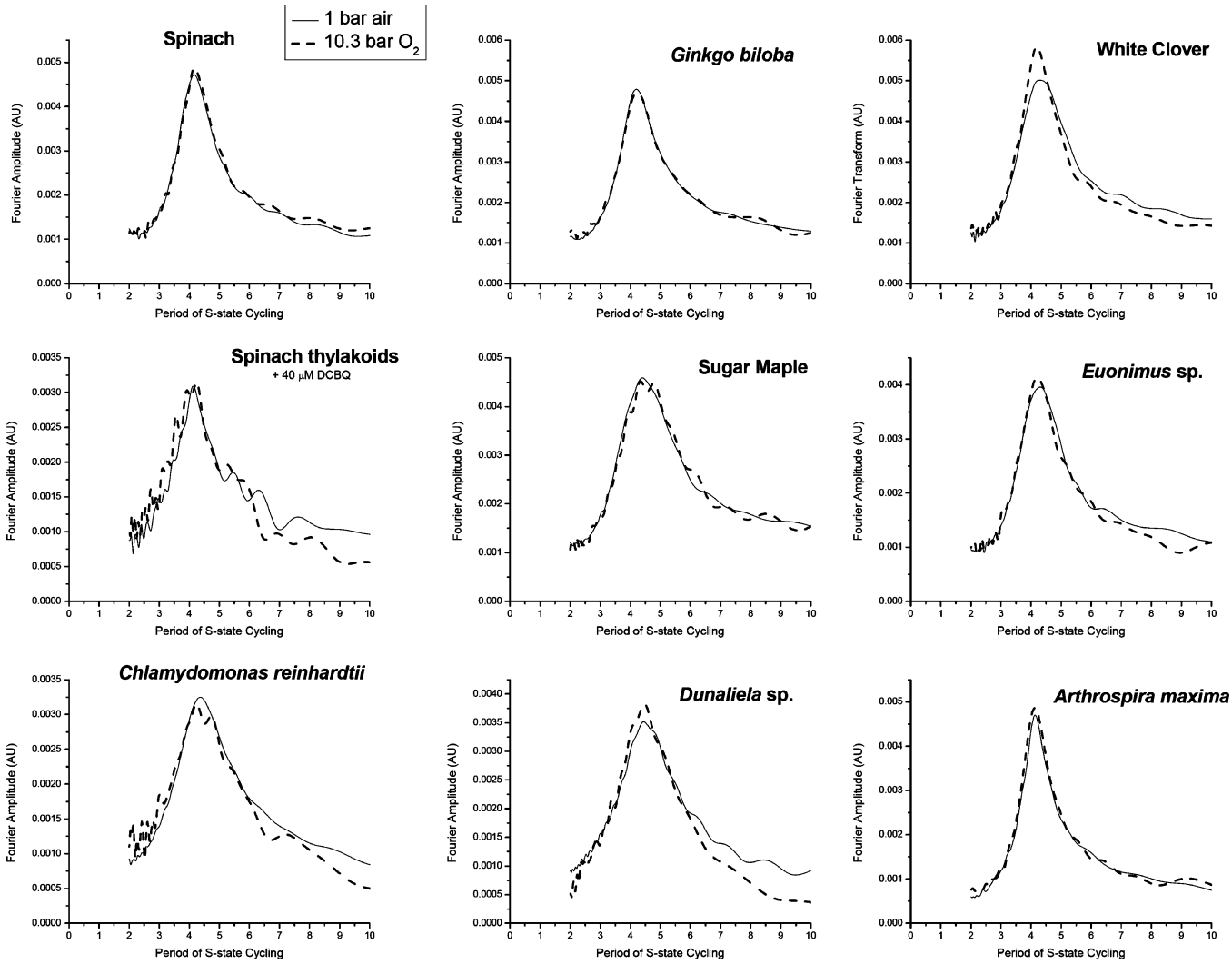

FIGURE 3: Fourier transformation of F_v/F_m data for organisms at 1 bar of air and 10.3 bar of O_2. Solid traces represent 1 bar of air, and dashed traces represent 10.3 bar of O_2. All data were treated as described in Experimental Procedures. Relative differences between the traces and respective normalization factors for each species are listed in Table 1.

Table 1: Changes in Oscillating Component of F_v/F_m Fourier Amplitude and Fourier Period Relative to Atmospheric Conditions[a]

organism	normalization factor[c]	Fourier amplitude change (%)[b]	period		
			1 bar of air	Δperiod	Δperiod (%)
Higher Plants (Leaves)					
Ginkgo biloba	1.05	−2	4.20	0.02	0.5
sugar maple	1.06	−4	4.40	0.17	3.9
Euonimus sp.	1.16	4	4.31	−0.1	−2.3
white clover	0.94	16	4.29	−0.16	−3.7
spinach	1.04	3	4.17	0.02	0.5
spinach thylakoids	1.41	0	4.14	−0.03	−0.7
Algae					
Dunaliela sp. CCMP 1320	2.18	9	4.44	−0.03	−0.7
C. reinhardtii cc124	1.92	−9	4.37	0.04	0.9
Cyanobacteria					
A. maxima (7 bar)	1.26	3	4.13	0.01	0.2
A. maxima	1.68	0	4.17	−0.05	−1.2
A. maxima (43 bar)	1.22	−3	4.36	−0.14	3.2

[a] Data at 10.3 bar except as noted. [b] Amplitude changes follow normalization. [c] Three-to-five flash normalization factor applied to data taken under elevated O_2.

The stability of the samples was monitored by integrating individual F_v/F_m flash sequences and plotting the sum of 50 flashes taken each 2 min, denoted integrated F_v/F_m, as a function of time over 24 h (Supporting Information, Figure S1). Samples under atmospheric conditions showed steady-state F_v/F_m (the nonoscillating component, which is approximately the F_v/F_m level during the final 10 flashes of the 50 flash measurements) that was either stable for 24 h (other than random noise around some basal level) or had a small and very slow rate of decay reflecting a variety of intrinsic factors, most notably photoreduction of the finite pool of electron acceptors (*21*). All organisms showed a more

rapid decay of the nonoscillating component of F_v/F_m over time when exposed to elevated levels of O_2 and light. Additionally, the rate of this decay was strongly species dependent. This decay was only observed when the samples were exposed to light and was not seen when samples were exposed to elevated levels of O_2 in the dark. Additional studies not reported here allowed us to attribute the decay of the nonoscillating component of F_v/F_m under elevated O_2 conditions to the production of oxygen-induced radicals via PSI-mediated photoreduction of O_2 (i.e., the Mehler reaction) (Kolling, Brown, Ananyev, and Dismukes, manuscript in preparation). This decay of the fluorescence signal over 24 h resulted in a relative loss of intensity of the oscillations in samples under elevated O_2 conditions versus those under atmospheric conditions (Supporting Information, Figure S7). The decay of the oscillations begins to occur after 0−4 h exposure to light and O_2 and depends upon the species (Supporting Information, Figure S2). This inactivation over hours is relatively slow compared to the damping of the oscillations. Although interesting, the focus of this study is the mechanism of water oxidation and not slow degradation of PSII turnover due to reactive oxygen species; therefore, here we focus on analyzing the changes in the oscillating component of F_v/F_m, which include changes in the rate of decay in the oscillations and the period.

Unlike the Kok model used for analyzing the S-state cycle (*11*), the Fourier transformation of the oscillations provides a model-independent approach to data presentation which eliminates the need for assumptions about the number of S-state cycle parameters and upon which S-states they act (*22, 23*). An increase in the rate of damping of the oscillations (loss of amplitude during the 50 flash measurement used for sampling the S-state cycle) will show up as an increase in the Fourier period. A comparison is shown of measurements taken at 1 bar of air vs 43 bar of oxygen for *A. maxima* in Figure 2. The raw data reveal there is about 25% loss in amplitude of the steady-state F_v/F_m level over the 2 h integration period, which is due to the aforementioned PSI-dependent Mehler reaction. All data were analyzed as shown in the example of *A. maxima* in Figure 2 and described in Experimental Procedures. Briefly, to directly compare the rate of damping of the oscillations, a spline fitting was first subtracted from both data sets, which removes the slowly decaying component of the steady-state F_v/F_m. Next, in order to compare the rate of damping of the oscillations, the data were normalized to the three-to-five peak intensity of the 1 bar air sample. Finally, a Fourier transformation is performed, and for this sample there is a small, 3.2%, increase in the oscillation frequency and a small, −3%, loss in the Fourier amplitude at 43 bar of oxygen versus 1 bar of air (210 × atmospheric pressure). This indicates that there is minimal difference in the rate of damping of oscillations under 43 bar of oxygen. Measurements taken at 7 and 10 bar of oxygen produce smaller shifts in the frequency equal to 0.2% and −1.2% with small changes in Fourier amplitude of 3% and 0%, respectively. From this, we learn that there are only small changes in the frequency of the S-state cycle, indicating minimal impact of oxygen pressure on the catalytic cycle of water oxidation for whole cells of *A. maxima*. In addition, oxygen pressure causes little, if any, change in the Fourier amplitude.

Similar results were observed for seven other species of algae and higher plants as shown in Figure 3 (raw data found in Supporting Information, Figure S3). Table 1 summarizes the relative changes in Fourier intensity and period of the oscillations (flash number). At 10 bar of O_2 there are only small changes in the period of oscillations ranging from −3.7% to +3.9% with a comparable distribution of positive and negative examples (Supporting Information, Figure S4). Comparison of all samples exposed to atmospheric conditions and 10 bar of O_2 shows that there may be a weak anticorrelation between the small changes in the Fourier amplitude and period. Specifically, the data show that a positive (negative) change in Fourier amplitude correlates with a negative (positive) shift in Fourier period (Supporting Information, Figure S4). We note that small nonsystematic differences in S-state cycle period are observed at atmospheric conditions which give a range of periods for any given type of sample (4.1−4.5 flash numbers). These variations arise from using field samples of different ages, physiological state, and prior history of the samples.

Interestingly, in the case of white clover, *Dunaliella* and *Euonimus*, 10 bar of O_2 pressure actually *increased* the initial amplitude of F_v/F_m and lowered the rate of damping of oscillations prior to the onset of slow O_2-induced photoinactivation. The former is revealed by increases of 16%, 9%, and 4% in the Fourier amplitude, respectively. There is also slightly slower damping of these three samples (S-states retain synchronization for a greater number of flashes) which shows up as a small decrease of the Fourier period of −3.7%, −0.7%, and −2.3%, respectively. This decrease in period corresponds to centers that approach the idealized response of four flashes expected for an S-state cycle without damping (*11*). We may attribute these simultaneous increases in the nonoscillating F_v/F_m level, Fourier amplitude, and reduced damping of the oscillating F_v/F_m signal to O_2-induced oxidation of a partially reduced electron acceptor pool (plastoquinone). An increase in Fourier amplitude can also arise due to a shift in the dark distribution of S-states from 25% S_0 + 75% S_1 in most dark-adapted OECs to 100% S_1, caused by oxidation of the metastable S_0-state (*11, 31*). In summary for these three samples, the OEC behaves as if elevated O_2 produces a more synchronized population of PSII centers with less damping.

A comparison of intact spinach leaves vs isolated thylakoid membranes reveals a loss of F_v/F_m intensity in thylakoids (Supporting Information, Figure S5). This arises from the limited electron acceptor capacity (plastoquinone pool size), which is partially lost upon isolation of thylakoids (*32*). The effect of 10 bar of O_2 pressure on spinach leaves and thylakoids was distinguishable, but insignificant; leaves and thylakoids exhibit small changes in Fourier period of +0.5% and −0.7%, respectively (Table 1).

DISCUSSION

Our studies show that there are only small direct effects of high O_2 pressure on the frequency and damping of the oscillations of the S-state cycle in intact cells and leaves sampled across cyanobacteria, algae, and higher plants. This demonstrates that the mechanism of the OEC S-state cycle is unaffected in the presence of elevated levels of O_2. The weak anticorrelation between the small changes in the Fourier amplitude and Fourier period and the small elevated initial level of F_v/F_m at 10 bar of O_2 can be attributed to known mechanisms that affect the electron acceptor pool or the

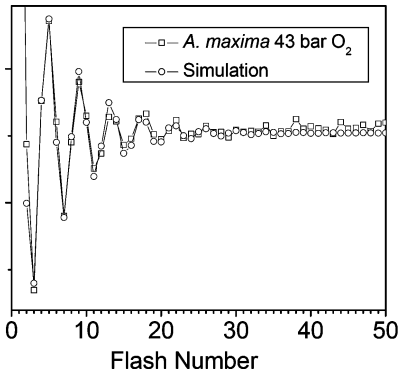

FIGURE 4: Simulated F_v/F_m data versus F_v/F_m data of *A. maxima* at at 43 bar of O_2. *A. maxima* F_v/F_m data were baselined with a cubic spline fitting (□). Simulated F_v/F_m data were generated as described in Experimental Procedures (○).

distribution of native S_0/S_1-states in the dark. In addition, we observed decreases in the nonoscillating component of the F_v/F_m signal intensity over time (on an hours scale) due to buildup of reactive O_2 species produced by PSI through a light-dependent mechanism (Kolling, Brown, Ananyev, Dismukes, manuscript in preparation). Our findings are consistent with several historical studies which show that atmospheric O_2 has little if any direct effect on photosynthetic electron transport and productivity other than secondary photoinactivation in some samples (*3*).

The absence of effect of 10 bar of O_2 pressure on the S-state cycle in spinach thylakoid membranes is noteworthy as membranes have reduced levels, if any at all, of respiratory enzymes that could lower intracellular O_2 concentration. This observation contrasts with that made by Clausen et al., who found, using detergent-extracted PSII protein and protein-enriched membrane complexes, that they were unable to perform multiple complete S-state cycles at even lower O_2 pressures (*1, 2*). In order to investigate this discrepancy further, we have performed simulations based upon two modified S-state models that would be expected if an inactivation or shunt phenomenon were present, similar to the model of Clausen et al. Next we describe these simulations and compare them to the data.

Simulated vs Real Photosynthetic Variable Fluorescence Data. Simulations were done using a simple Markov model that predicts S-state populations as a function of single-turnover flash number (see Experimental Procedures). Figure 4 shows the comparison between real and simulated F_v/F_m data as a function of single-turnover flashes for *A. maxima* at atmospheric pressure (Supporting Information, Figure S6, shows comparisons of simulations to F_v/F_m in other species). For comparison to the real data, the simulated data were processed by using the same method described in Experimental Procedures and shown in Figure 2; notably, this also includes the three-to-five flash amplitude normalization. The sum of the S_0- and S_1-state populations was found to accurately predict the F_v/F_m oscillations found in all of the samples, as previously described for *A. maxima* in air (*21*).

Shunt Simulation. Perturbations to the S-state populations in a normal Kok model were calculated by addition of a shunt with the S_3-state proceeding directly to the S_2-state. This model also includes the possibility of a shunt occurring from the S_4-state (see Figure 1A); therefore, the shunt postulated by Clausen and Junge and later supported by Clausen et al. is also described by this shunt simulation (*1, 2*). Figure 5A,C,E shows the results of the shunt simulation as a function of the percent of the PSII centers participating in the shunt. The simulated data correspond to the optimal fitting of the real data using the analytical solution to the Kok model (parameters: $\alpha = 0.12$; $\beta = 0.03$; initial $S_0 = 0.25$; initial $S_1 = 0.75$). The rate of damping of the oscillations becomes greater during each 50 flash simulation, and the Fourier amplitude of the period four peak decreases, respectively. Upon 100% of photocenters experiencing the shunt, the signal is similar to a DCMU-treated sample (blocks Q_A^- reoxidation) in which most photocenters are blocked after one flash and no longer contribute to variable fluorescence (Supporting Information, Figure S7).

Fourier transformation of the shunt model populations shows that as the effect of the shunt becomes greater, the period of the oscillations shift slightly to a greater number of flashes ($\Delta = 0.09$ (2%) when 50% of the centers experience a shunt). In other words, as the shunt becomes more prevalent, more flashes are needed to cycle the system through the S_0-state. This positive shift is not large enough to use as a definitive metric for the presence of the shunt in actual systems, as the predicted shift generally falls within the range of shifts expected from other sources as described above. By contrast, the model predicts a large acceleration in the loss of the oscillating amplitude of F_v/F_m as more centers are affected by the shunt; this effect is significant and can be used as a metric (Figure 5E). It should be clear that a system with a shunt should follow the trend predicted by the simulations.

This shunt simulation does not account for the possibility that an intermediate generated during the S_3-state to S_0-state transition would result in a higher level of fluorescence. It is reasonable to assume that the formation of $S_2^*(H_2O_2)$ would lead to a higher level of fluorescence as the formation of H_2O_2 requires more energy than forming O_2, but the intensity of such change is difficult to predict, and its inclusion into the simulations would be problematic due to the vast number of trials that would have to be performed to explore this possibility. A noticeable change in the level of fluorescence due to this intermediate would lead to a shift in the period of the oscillations and would be noticeable in our data. Since we did not observe any large shifts or formation of new peaks in our F_v/F_m data, there was no reason to attempt further simulations.

Inactivation Simulation. Simulations were performed to determine what would happen to S-state populations if an inactivation occurred following the S_3-state. We modeled this inactivation by removing a percentage of PSII centers from the PSII population being measured after they reached the S_3-state. This simulation addresses the case, as suggested by Clausen and Junge and Clausen et al., in which PSII centers in the hypothetical $S_2^*(H_2O_2)$ state are stabilized for the duration of the measurement (see Figure 1). These centers would no longer contribute to the F_v/F_m measurement and, hence, appear inactivated. It should also be noted that inactivation of the S-state cycle by trapping the S_3-state, S_4-state, or any intermediates during the terminal reaction ($S_4 \rightarrow S_0$) would be accurately described by this simulation.

Figure 5B,D,F shows the results of the inactivation at any point within $S_3 \rightarrow S_0$ on the $S_0 + S_1$ populations and the corresponding Fourier transform, respectively; individual

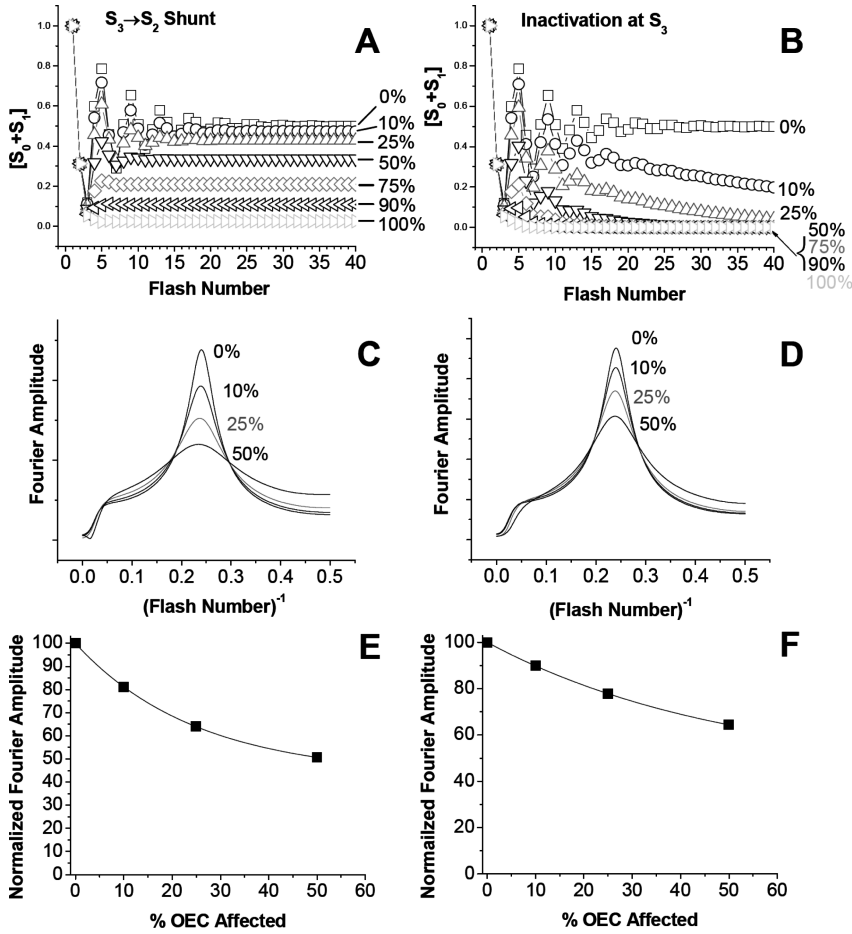

FIGURE 5: Simulated F_v/F_m data for the shunt and inactivation models. (A, C, E) Simulated F_v/F_m data for the $S_3 \rightarrow S_2$ shunt model. (B, D, F) Simulated F_v/F_m data for the inactivation model. Simulated data were generated and analyzed as described in Experimental Procedures with the following parameters: $\alpha = 0.10$; $\beta = 0.05$; initial $S_0 = 0.25$; initial $S_1 = 0.75$. (A, B) Population of $S_0 + S_1$ states. (C, D) Fourier transformation of the simulated F_v/F_m data following normalization to the three-to-five flash peak of the 0% trace. (E, F) Fourier amplitude decay as a function of % of centers affected.

traces show conditions under which a certain percentage of centers are inactivated during a single PSII turnover. As a greater percentage of the PSII centers are subjected to an inactivation event, the intensity of the oscillations decreases as a simple first-order exponential decay function.

The Fourier transformation shows that as the percent of centers contributing to the inactivation becomes greater, the period of the oscillations shifts slightly to greater number of flashes ($\Delta = 0.02$ at 50% effect) but not as much as described previously for the period of the shunted model. By contrast, the predicted large decrease in Fourier amplitude can be used as a metric for this model.

Analysis of Models. Comparison of the models to the experimental results in Table 1 reveals that only data for sugar maple (10 bar), *C. reinhardtii* (10 bar), and *A. maxima* (43 bar) show both positive shift in Fourier period and loss of Fourier amplitude larger than random error, as predicted by both models. However, these changes are relatively small. *C. reinhardtii* showed the most pronounced decrease in its Fourier amplitude at 9%, accompanied by a very small 0.9% increase in period. The shunt model simulation predicts that an ~19% decrease in Fourier amplitude would occur for a 10% shunt effect. The inactivation model simulation predicts a 10% amplitude decrease for a 10% inactivation effect. Thus, at best these models could account for the response of only 5% and 9% of PSII centers in *C. reinhardtii,* respectively. None of the other seven distinct organisms exhibit blockage in S-state cycling at elevated O_2.

In the event of a shunt with the S_3-state proceeding directly to the S_2-state, one might expect to see a period two oscillation as the PSII centers would only need two flashes to turnover. This effect was not observed in the simulations and is a result of the fact that one observes a high level of fluorescence on the S_0-state to S_1-state and S_1-state to S_2-state transition while fluorescence is largely quenched on the S_2-state to S_3-state and S_3-state to S_0-state transition (Figure 1). The S_3-state to S_2-state shunt would result only in the third and fourth transitions of the S-state cycle, which would no longer result in an oscillation pattern.

Clausen and Junge and Clausen et al. (*1, 2*) determined that the O_2-induced blockage of S-state cycling in isolated PSII centers reached its half-maximum point at 2.3 bar of O_2. On the basis of these works, we should expect to see a 75% blockage in our samples exposed to 10.3 bar of O_2. Even our measurements at 43 bar with whole cells of *A. maxima* failed to reveal a significant blockage in S-state cycling. Our results do not resolve the origin of the effect they reported, although it may be a result of their using detergent-extracted PSII particles.

In conclusion, photosynthetic cells are known to be sensitive to damage caused by illumination in the presence of O_2. Oxygen accelerates the rate of damage to whole cells and leaves upon

illumination at a site that involves superoxide formed at PSI and by reactive O_2 species production. However, the present results establish that S-state cycling within the OEC of native leaves and cells from both prokaryotic and eukaryotic oxygenic phototrophs is insensitive to O_2 pressure up to 50 times current atmospheric partial pressure (215× in *A. maxima*). We investigated two models for inactivation of S-state cycling which reveal distinctly different deactivation patterns of S-state populations, which were used to assess the sensitivity of the experimental method (*14, 15*). From this we may conclude that the energetics of the terminal step, $S_3 \rightarrow S_0 + O_2 + e^- + nH^+$, are sufficiently exoergic that the release of O_2 cannot be prevented. This result does not mean that a peroxo species does not form during this transition, as there are sound energetic reasons for predicting this as intermediate (*16, 17*), rather that it cannot be trapped by shifting the equilibrium. These results have implications for models of how oxygenic photosynthesis may have evolved in earlier geological epochs.

ACKNOWLEDGMENT

We thank Paul Falkowski for ECCMP 1320 and Peter Wu for preliminary simulations.

SUPPORTING INFORMATION AVAILABLE

Supporting figures as described in the text. This material is available free of charge via the Internet at http://pubs.acs.org.

REFERENCES

1. Clausen, J., and Junge, W. (2004) Detection of an intermediate of photosynthetic oxygen evolution. *Nature 430*, 480–484.
2. Clausen, J., Junge, W., Dau, H., and Haumman, M. (2005) Photosynthetic water oxidation at high O_2 backpressure monitored by delayed chlorophyll fluorescence. *Biochemistry 44*, 12775–12779.
3. Raven, J. A., and Larkum, A. W. D. (2007) Are there ecological implications for the proposed energetic restrictions on photosynthetic oxygen evolution at high oxygen concentrations? *Photosynth. Res. 94*, 31–42.
4. Dau, H., and Haumann, M. (2006) Photosynthetic oxygen production—Response. *Science 312*, 1471–1472.
5. Junge, W., and Clausen, J. (2006) Photosynthetic oxygen production. *Science 312*, 1470–1470.
6. Penner-Hahn, J. E., and Yocum, C. F. (2006) Photosynthetic oxygen production—Response. *Science 312*, 1470–1471.
7. Dismukes, G. C., and Blankenship, R. E. (2005) The Origin and Evolution of Photosynthetic Oxygen Production, in *Photosystem II: The Water/Plastoquinone Oxido-Reductase in Photosynthesis* (Wydrzynski, T., and Satoh, K., Eds.) pp 683−695, Springer, Amsterdam, The Netherlands.
8. Chisti, Y. (2007) Biodiesel from microalgae. *Biotechnol. Adv. 25*, 294–306.
9. Kreslavski, V. D., Carpentier, R., Klimov, V. V., Murata, N., and Allakhverdiev, S. I. (2007) Molecular mechanisms of stress resistance of photosynthetic apparatus. *Biol. Membr. 24*, 195–217.
10. Joliot, P., Barbieri, G., and Chabaud, R. (1969) A new model of photochemical centers in system-2. *Photochem. Photobiol. 10*, 309–329.
11. Kok, B., Forbush, B., and McGloin, M. (1970) Co-operation of charges in photosynthetic O_2 evolution. I. A linear four step mechanism. *Biochim. Biophys. Acta 11*, 467–475.
12. Haumann, M., Liebisch, P., Müller, C., Barra, M., Grabolle, M., and Dau, H. (2005) Photosynthetic O_2 formation tracked by time-resolved X-ray experiments. *Science 310*, 1019–1021.
13. Haumann, M., Bogershausen, O., Cherepanov, D. A., Ahlbrink, R., and Junge, W. (1997) Photosynthetic oxygen evolution: H/D isotope effects and the coupling between electron and proton transfer during the redox reactions at the oxidizing side of photosystem II. *Photosynth. Res. 51*, 193–208.
14. Renger, G. (1997) Mechanistic and structural aspects of photosynthetic water oxidation. *Physiol. Plant. 100*, 828–841.
15. Krishtalik, L. I. (1990) Activation energy of photosynthetic oxygen evolution: an attempt at theoretical analysis. *Bioelectrochem. Bioenerg. 23*, 249–263.
16. Renger, G. (1977) Model for molecular mechanism of photosynthetic oxygen evolution. *FEBS Lett. 81*, 223–228.
17. Ananyev, G., Wydrzynski, T., Renger, G., and Klimov, V. (1992) Transient peroxide formation by the manganese-containing, redox-active donor side of photosystem-II upon inhibition of O_2 evolution with lauroylcholine chloride. *Biochim. Biophys. Acta 1100*, 303–311.
18. Dismukes, G. C., Zheng, M., Hutchins, R., and Philo, J. S. (1994) The inorganic biochemistry of photosynthetic water oxidation. *Biochem. Soc. Trans. 22*, 323–327.
19. Berthold, D. A., Babcock, G. T., and Yocum, C. F. (1981) A highly resolved, oxygen-evolving photosystem-II preparation from spinach thylakoid membranes—Electron-paramagnetic-res and electron-transport properties. *FEBS Lett. 134*, 231–234.
20. Ananyev, G. M., and Dismukes, G. C. (1996) Assembly of the tetra-Mn site of photosynthetic water oxidation by photoactivation: Mn stoichiometry and detection of a new intermediate. *Biochemistry 35*, 4102–4109.
21. Ananyev, G., and Dismukes, G. C. (2005) How fast can photosystem II split water? Kinetic performance at high and low frequencies. *Photosynth. Res. 84*, 355–365.
22. Shinkarev, V. (2003) Oxygen evolution in photosynthesis: Simple analytical solution for the Kok model. *Biophys. J. 85*, 435–441.
23. Shinkarev, V. (2005) Flash-induced oxygen evolution in photosynthesis: Simple solution for the extended S-state model that includes misses, double hits, inactivation, and backwards transitions. *Biophys. J. 88*, 412–421.
24. Shinkarev, V. P. (2005) Flash-Induced Oxygen Evolution and Other Oscillation Processes in Photosystem II, in *Photosystem II: The Water/Plastoquinone Oxido-Reductase in Photosynthesis* (Wydrzynski, T., and Satoh, K., Eds.) pp 539−565, Springer, Amsterdam, The Netherlands.
25. Dau, H. (1994) Molecular mechanisms and quantitative models of variable photosystem-II fluorescence. *Photochem. Photobiol. 60*, 1–23.
26. Delosme, R., and Joliot, P. (2002) Period four oscillations in chlorophyll a fluorescence. *Photosynth. Res. 73*, 165–168.
27. Shinkarev, V. P. (2004) Photosystem II: Oxygen Evolution and Chlorophyll *a* Fluorescence Induced by Multiple Flashes, in *Chlorophyll a Fluorescence: A Signature of Photosynthesis* (Papageorgiou, G. C., and Govindjee, Eds.) pp 197−229, Springer, Norwell, MA.
28. Nedbal, L., and Koblizek, M. (2006) Chlorophyll Fluorescence as a Reporter on in Vivo Electron Transport and Regulation in Plants, in *Chlorophylls and Bacteriochlorophylls* (Grimm, B., Porra, R. J., Rudiger, W., and Scheer, H., Eds.) pp 507−519, Springer, Dordrecht, The Netherlands.
29. Kolber, Z. S., Prasil, O., and Falkowski, P. G. (1998) Measurements of variable chlorophyll fluorescence using fast repetition rate techniques: defining methodology and experimental protocols. *Biochim. Biophys. Acta 1367*, 88–106.
30. Taoka, S., Jursinic, P. A., and Seibert, M. (1993) Slow oxygen release on the first 2 flashes in chemically stressed photosystem-II membrane-fragments results from hydrogen-peroxide oxidation. *Photosynth. Res. 38*, 425–431.
31. Styring, S., and Rutherford, A. W. (1987) In the oxygen-evolving complex of photosystem-II the S_0 state is oxidized to the S_1 state by D^+ (Signal-Iislow). *Biochemistry 26*, 2401–2405.
32. Renger, G., and Schulze, A. (1985) Quantitative-analysis of fluorescence induction curves in isolated spinach-chloroplasts. *Photobiochem. Photobiophys. 9*, 79–87.

BI801774F